


NANO IDEA

Open Access



# A Facile Method for Loading CeO<sub>2</sub> Nanoparticles on Anodic TiO<sub>2</sub> Nanotube Arrays

Yulong Liao<sup>1,2\*</sup> , Botao Yuan<sup>1</sup>, Dainan Zhang<sup>1</sup>, Xiaoyi Wang<sup>1</sup>, Yuanxun Li<sup>1</sup>, Qiye Wen<sup>1</sup>, Huaiwu Zhang<sup>1</sup> and Zhiyong Zhong<sup>1</sup>

## Abstract

In this paper, a facile method was proposed to load CeO<sub>2</sub> nanoparticles (NPs) on anodic TiO<sub>2</sub> nanotube (NT) arrays, which leads to a formation of CeO<sub>2</sub>/TiO<sub>2</sub> heterojunctions. Highly ordered anatase phase TiO<sub>2</sub> NT arrays were fabricated by using anodic oxidation method, then these individual TiO<sub>2</sub> NTs were used as tiny “nano-containers” to load a small amount of Ce(NO<sub>3</sub>)<sub>3</sub> solutions. The loaded anodic TiO<sub>2</sub> NTs were baked and heated to a high temperature of 450 °C, under which the Ce(NO<sub>3</sub>)<sub>3</sub> would be thermally decomposed inside those nano-containers. After the thermal decomposition of Ce(NO<sub>3</sub>)<sub>3</sub>, cubic crystal CeO<sub>2</sub> NPs were obtained and successfully loaded into the anodic TiO<sub>2</sub> NT arrays. The prepared CeO<sub>2</sub>/TiO<sub>2</sub> heterojunction structures were characterized by a variety of analytical technologies, including XRD, SEM, and Raman spectra. This study provides a facile approach to prepare CeO<sub>2</sub>/TiO<sub>2</sub> films, which could be very useful for environmental and energy-related areas.

**Keywords:** Anodic TiO<sub>2</sub> nanotubes, CeO<sub>2</sub> nanoparticles, CeO<sub>2</sub>/TiO<sub>2</sub> heterojunctions, Green chemistry

## Background

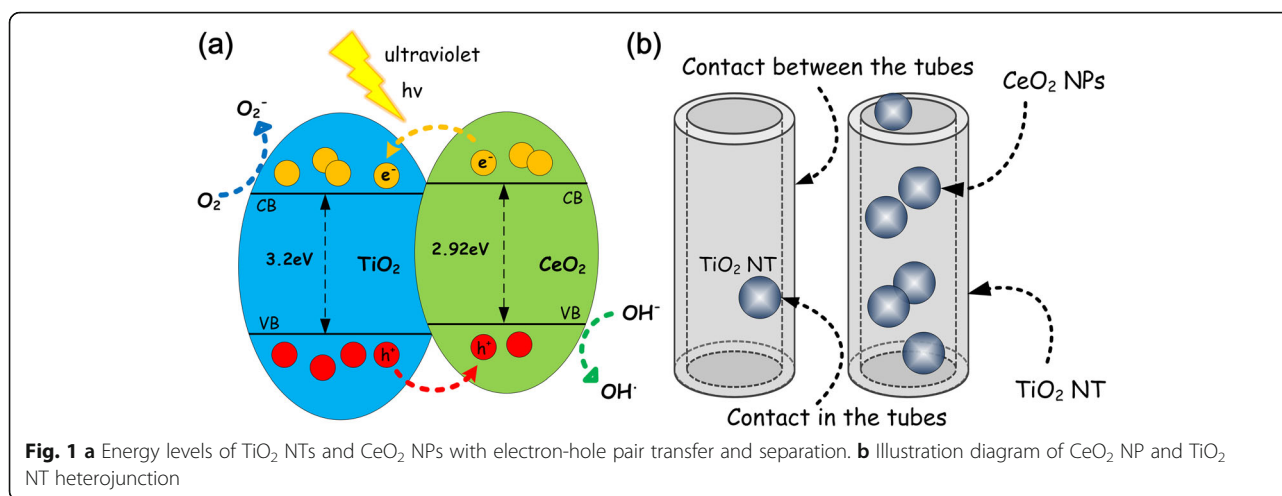
As is well known, titanium dioxide (TiO<sub>2</sub>) materials have been widely used for a great number of applications such as solar cells, water treatment materials, catalysts and so on [1–6]. The reason for TiO<sub>2</sub> and TiO<sub>2</sub>-derived materials have so many applications is they have outstanding photocatalytic, electrical, mechanical, and thermal properties [7–9]. In nature, TiO<sub>2</sub> has three most commonly encountered crystalline polymorphs, including anatase, rutile, and brookite. Among the three TiO<sub>2</sub> polymorphs, anatase is the most photoactive polymorph used for degradation of organic pollutants or electrodes for energy applications [10, 11]. Anatase TiO<sub>2</sub> have a band gap of ~ 3.2 eV, and it has shown good catalytic activity, corrosion resistance, and light resistance. Along with its stable performance, low cost, non-toxic harmless, TiO<sub>2</sub> in anatase phase was recognized as the best photocatalyst.

Recently, TiO<sub>2</sub> nanotube (NT) arrays have attracted great attention due to its unique tubular structure-induced advantages [12–18]. However, their performances were still limited by inherent material faults, such as relatively wide gaps (~ 3.2 eV) [19–22]. In order to achieve better application, narrow band semiconductors with proper energy level were proposed to further modify TiO<sub>2</sub> NT arrays [23, 24]. The band gap of cubic CeO<sub>2</sub> is about 2.92 eV and has good chemical stability. TiO<sub>2</sub> modified by CeO<sub>2</sub> were found very useful in the field of photocatalysis, gas sensors, and so on [25–27]. In the field of photocatalysis, the rapid recombination of photogenerated electron-hole pairs of reduces the photocatalytic performance of TiO<sub>2</sub>. However, the modification of CeO<sub>2</sub> changes the recombination rate of the electron-hole pairs inside a CeO<sub>2</sub>/TiO<sub>2</sub> composite material. As shown in the Fig. 1a, once CeO<sub>2</sub>/TiO<sub>2</sub> heterojunctions are formed, more superoxide and hydroxyl radicals could be produced, leading to improved photocatalytic performance. In the field of gas sensors, CeO<sub>2</sub> is a promising material for oxygen gas sensing at high temperature. TiO<sub>2</sub> modified by CeO<sub>2</sub> could effectively improve the adaptability of gas sensor, because the CeO<sub>2</sub>/TiO<sub>2</sub> heterostructures enable the sensing of oxygen gas at low operating

\* Correspondence: [yulong.liao@uestc.edu.cn](mailto:yulong.liao@uestc.edu.cn)

<sup>1</sup>State Key Laboratory of Electronic Thin Film and Integrated Devices, University of Electronic Science and Technology of China, Chengdu 610054, China

<sup>2</sup>Center for Applied Chemistry, University of Electronic Science and Technology of China, Chengdu 610054, China



temperatures ( $< 500^\circ\text{C}$ ) [28]. In order to prepare  $\text{CeO}_2/\text{TiO}_2$  heterostructures, many approaches have been proposed including sol-gel method and hydrothermal method [29–31]. The former works were found very interesting and their products had shown good performances. However, the traditional methods are always used to prepare  $\text{CeO}_2/\text{TiO}_2$  heterostructures in powder form and often with complicated procedures. For preparing  $\text{CeO}_2/\text{TiO}_2$  heterostructures based on  $\text{TiO}_2$  NTs as shown in Fig. 1b, developing facile method to load  $\text{CeO}_2$  nanoparticles (NPs) on the  $\text{TiO}_2$  NT arrays is highly desired. To this end, we proposed a novel method for the preparation of  $\text{CeO}_2/\text{TiO}_2$  heterojunctions in this study.

Highly ordered anatase phase  $\text{TiO}_2$  NT arrays were fabricated by anodic oxidation method, then the individual  $\text{TiO}_2$  NTs were prepared as tiny “nano-containers” to load  $\text{Ce}(\text{NO}_3)_3$  solutions. The loaded anodic  $\text{TiO}_2$  NTs were heated to a high temperature, under which the  $\text{Ce}(\text{NO}_3)_3$  were thermal decomposed. After the thermal decomposition of  $\text{Ce}(\text{NO}_3)_3$ , cubic crystal  $\text{CeO}_2$  NPs were obtained and successfully loaded into the anodic  $\text{TiO}_2$  NT arrays.  $\text{CeO}_2/\text{TiO}_2$  heterojunctions prepared by this method was recognized as simple operation, low cost, non-toxic harmless.

## Experimental Section

### Synthesis of $\text{TiO}_2$ Nanotube Arrays

Firstly, we used anodic oxidation method to prepare  $\text{TiO}_2$  nanotube arrays [32–34]. Briefly, titanium pieces were cut into small pieces ( $5\text{ cm} \times 1.5\text{ cm}$ ) and flattened. After being washed in detergent water, the titanium pieces were washed in an ultrasonic cleaner for 1 h with deionized water and alcohol, respectively. The dried titanium sheets with a counter electrode were immersed in the prepared electrolyte (500 ml glycol, 10 ml  $\text{H}_2\text{O}$  and 1.66 g  $\text{NH}_4\text{F}$ ) under room temperature. A constant voltage of 60 V was applied to the two electrodes for

2 h. Then,  $\text{TiO}_2$  NT films were annealed at  $450^\circ\text{C}$  for 3 h, and the rate of anatase  $\text{TiO}_2$  NTs were obtained.

### Synthesis of $\text{CeO}_2/\text{TiO}_2$ Heterojunction

The individual  $\text{TiO}_2$  NTs inside the anodic films were taken as thousands small nano-containers to load the raw materials of  $\text{CeO}_2$ , which will be full with the Ce contained solutions. As shown in Fig. 2, the  $\text{TiO}_2$  NTs were immersed in the  $\text{Ce}(\text{NO}_3)_3$  solution (concentration were 0.05, 0.1, 0.2, 0.5, and 1 mol/L respectively) for 3 s. In order to ensure the open tube mouth of the  $\text{TiO}_2$  NTs, it is worthy of attention that superfluous solution on the surface of the  $\text{TiO}_2$  NT films should be absorbed by using a qualitative filter paper immediately. The films were tilted as much as possible, making the solution flow to the edge of the films, and the filter paper was used to dry out the superfluous solution to ensure uniformity of solution. Then, the loaded films were dried at  $70^\circ\text{C}$  for 1 h, during which the  $\text{Ce}(\text{NO}_3)_3$  solute will be deposited inside the  $\text{TiO}_2$  NT nano-containers. And the dried films were further annealed at  $450^\circ\text{C}$  for 2 h, during which the deposited  $\text{Ce}(\text{NO}_3)_3$  will be thermally decomposed into  $\text{CeO}_2$  NPs at a high temperature. Finally,  $\text{CeO}_2$  NPs were obtained and attached to each single  $\text{TiO}_2$  NT of the arrays.

### Characterization

Crystalline structure of the  $\text{CeO}_2/\text{TiO}_2$  heterojunction was analyzed by X-ray diffraction (XRD; D/max 2400 X Series X-ray diffractometer). XRD was applied to characterize the samples at a step of  $0.03^\circ$  in the range of  $10^\circ$  to  $80^\circ$ . The microstructure of the heterojunctions and the morphology of the nanotubes were characterized by scanning electron microscopy (SEM; JSM-7000F, JEOL Inc. Japan). The elemental distribution of the microscopic region of the materials was qualitatively and quantitatively analyzed by energy-dispersive spectrometry (EDS). The crystal structure of the

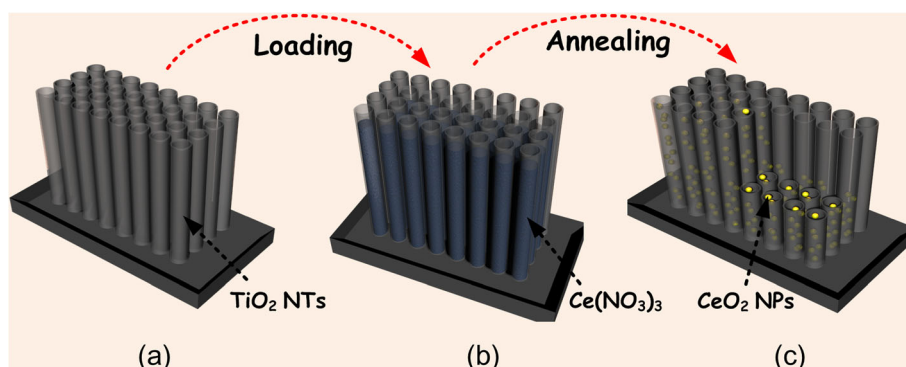


**Fig. 2** Synthesis flow of CeO<sub>2</sub>/TiO<sub>2</sub> heterojunction: (a) preparation of empty TiO<sub>2</sub> NTs, (b) loading the TiO<sub>2</sub> NTs with Ce(NO<sub>3</sub>)<sub>3</sub> solution, and (c) formation of CeO<sub>2</sub>/TiO<sub>2</sub> heterojunction structures

CeO<sub>2</sub>/TiO<sub>2</sub> heterojunction was also analyzed by Raman spectra (inVia, Renishaw, UK). Resonant Raman scattering spectra were recorded at room temperature to obtain a more clear display of components.

## Results and Discussion

### Crystalline Properties of the Prepared CeO<sub>2</sub>/TiO<sub>2</sub> Heterojunction Films

XRD patterns of the prepared CeO<sub>2</sub>/TiO<sub>2</sub> heterojunction films are shown in Fig. 3. The diffraction peak could be identified as the anatase phase of TiO<sub>2</sub> and cubic phase of CeO<sub>2</sub>. The diffraction peaks located at 25.28°, 36.80°, 37.80°, 48.05°, 53.89°, 55.06°, 62.68°, 70.30°, 75.03°, and 76.02° were attributed to the anatase lattice plane (101), (103), (004), (200), (105), (211), (204), (220), (215), and (301), respectively. Moreover, the minor diffraction peaks at 40.1° and 53.0° were attributed to (101) and (102) of Ti (see Fig. 3a). This indicates the anodic TiO<sub>2</sub>

NT films have an anatase crystalline structure in this study. In the crystallization process, anatase grains usually have a smaller size and a larger specific surface area. Therefore, anatase TiO<sub>2</sub> surface has strong adsorption capacity of H<sub>2</sub>O, O<sub>2</sub>, and OH<sup>−</sup> and its photocatalytic activity is greatly high [35, 36]. The adsorption capacity of the anatase TiO<sub>2</sub> NT films is enormously influenced in the photocatalytic reaction, and the strong adsorption capacity is beneficial to its activity. Meanwhile, the diffraction peak located at 28.55° and 33.08° was indexed to crystal face (111) and (200) of CeO<sub>2</sub>, respectively [37, 38]. Figure 3b shows the XRD patterns of the CeO<sub>2</sub>/TiO<sub>2</sub> heterojunction films with different initial Ce(NO<sub>3</sub>)<sub>3</sub> concentration. When the concentration of Ce(NO<sub>3</sub>)<sub>3</sub> was too low, only diffraction peaks of the anatase TiO<sub>2</sub> could be observed. With the concentration of Ce(NO<sub>3</sub>)<sub>3</sub> gradually increasing, the cubic phase of cerium oxide appeared and the diffraction peaks of cubic

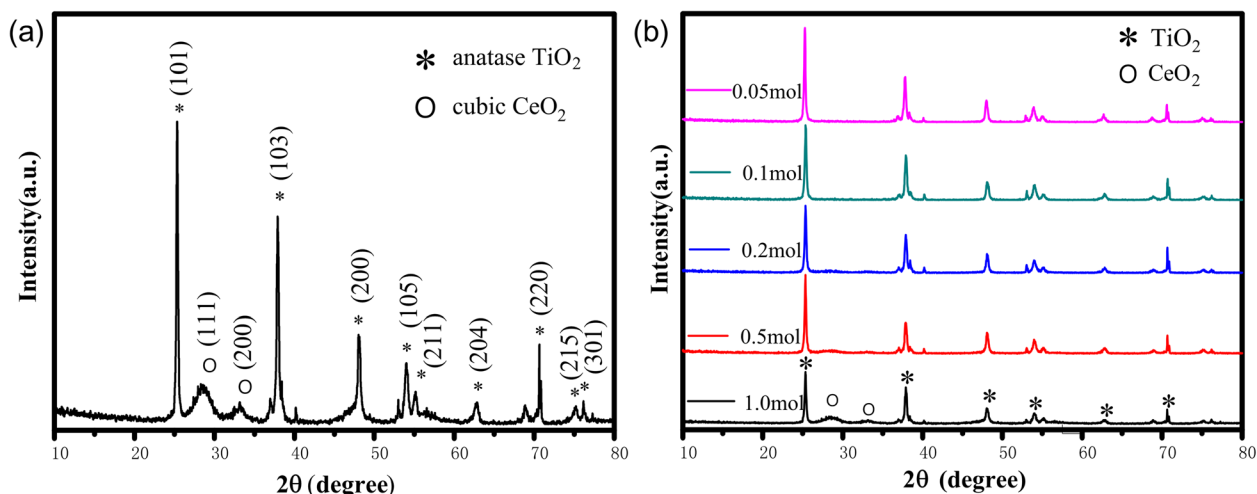


**Fig. 3** a XRD pattern of the anatase phase of TiO<sub>2</sub> and cubic CeO<sub>2</sub>. b XRD pattern of the anatase phase of TiO<sub>2</sub> and cubic CeO<sub>2</sub> with different concentrations of Ce(NO<sub>3</sub>)<sub>3</sub>

CeO<sub>2</sub> became stronger. According to the tested XRD data, the standard PDF showed CeO<sub>2</sub> has a face-centered cubic (FCC) crystal structure. The calculated lattice parameters were  $a = b = c = 0.5411$  nm and  $\alpha = \beta = \gamma = 90^\circ$ , which matched with the standard PDF. It could be summarized that TiO<sub>2</sub> was modified by CeO<sub>2</sub> perfectly in lattice matching so that their heterojunctions are tighter and better to produce a special electron transfer process which is able to facilitate the separation of the electron/hole pairs.

#### Microscopic Morphologies of the CeO<sub>2</sub>/TiO<sub>2</sub> Heterojunction Films

Figure 4 shows SEM images of the anatase TiO<sub>2</sub> nanotube arrays before and after being modified by CeO<sub>2</sub>. Top profile of the TiO<sub>2</sub> NT arrays without loading CeO<sub>2</sub> is shown as Fig. 4a, and the self-organized NT arrays were found quite dense and had an open-mouth top morphology, which provides a passage way for the Ce(NO<sub>3</sub>)<sub>3</sub> solution filling into the NTs in this study. The average tube diameter is evaluated about 110 nm. Figure 4b shows the microstructure of anodic TiO<sub>2</sub> NTs modified by CeO<sub>2</sub> NPs. It can be seen that there are lots of long strips on the tube-pore mouths by comparing to the pure TiO<sub>2</sub> NTs. Meanwhile, the tube wall thickness could be found getting increased by taking a close look. These observations indicate that the morphologies of the anodic TiO<sub>2</sub> NT arrays have an obvious change after the loading and annealing process. Also, from the SEM images, most CeO<sub>2</sub> NPs were deposited on the top of the TiO<sub>2</sub> NTs, because when the superfluous Ce(NO<sub>3</sub>)<sub>3</sub> solution was treated, the superfluous solution on the top of tubes was not completely disposed, and after thermally decomposed, the CeO<sub>2</sub> NPs were deposited on the top of tubes. Morphologies of the CeO<sub>2</sub>/TiO<sub>2</sub> heterojunction films with Ce(NO<sub>3</sub>)<sub>3</sub> solution concentration varying from 0.05 mol to 0.5 mol are shown in Fig. 5. It could be clearly seen that with the Ce(NO<sub>3</sub>)<sub>3</sub> solution concentration increasing, the nanoparticles in the TiO<sub>2</sub> NTs gradually became more abundant and more

elongated particles appeared on the TiO<sub>2</sub> NTs. These results reveal that the CeO<sub>2</sub> nanoparticles are successfully attached to tube wall of the anodic TiO<sub>2</sub> NT arrays, forming a CeO<sub>2</sub>/TiO<sub>2</sub> heterojunction structure. The large specific surface area of the TiO<sub>2</sub> NTs provides a good substrate for CeO<sub>2</sub> NPs to load onto the anodic TiO<sub>2</sub> NT films.

#### Components Analysis of the CeO<sub>2</sub>/TiO<sub>2</sub> Heterojunction Films

In order to coordinate with the SEM test results, energy-dispersive X-ray spectroscopy (EDS) was used to analyze the elemental composition of the CeO<sub>2</sub>/TiO<sub>2</sub> heterojunction films. EDS comparison diagram between TiO<sub>2</sub> NTs and CeO<sub>2</sub>/TiO<sub>2</sub> heterojunction is shown in Fig. 6. As shown in the Fig. 6a, only Ti and O could be detected. The atomic percentage of Ti and O elements is 27.37 and 65.36%, respectively. The sample of CeO<sub>2</sub>/TiO<sub>2</sub> heterojunction film which is prepared in the 0.1 mol/L Ce(NO<sub>3</sub>)<sub>3</sub> solution is shown in Fig. 6b. Ce, O, and Ti could be detected. The atomic percentage of Ce, Ti, and O elements is 11.91, 12.04, and 59.98%, respectively. It can be concluded from the EDS results that CeO<sub>2</sub> NPs were successfully deposited on the TiO<sub>2</sub> NTs.

In order to further investigate the obtained films, Raman spectroscopy was used to analyze the properties of the CeO<sub>2</sub>-loaded TiO<sub>2</sub> film. Figure 7 shows two typical Raman spectra of the pure anodic TiO<sub>2</sub> film and the CeO<sub>2</sub>/TiO<sub>2</sub> heterojunction film which is prepared in the 1 mol/L Ce(NO<sub>3</sub>)<sub>3</sub> solution. Peaks located at around 400, 530, and 645 cm<sup>-1</sup> could be clearly observed, which could be attributed to anatase TiO<sub>2</sub> phase. Along with these characteristic peaks of anatase TiO<sub>2</sub>, there is a new peak at about 460 cm<sup>-1</sup> that could be observed for the CeO<sub>2</sub>/TiO<sub>2</sub> films. According to the Raman-active mode, this peak could be ascribed to the cubic phase of CeO<sub>2</sub> [39]. The Raman spectra results also confirm that the CeO<sub>2</sub>/TiO<sub>2</sub> heterojunction was successfully prepared.

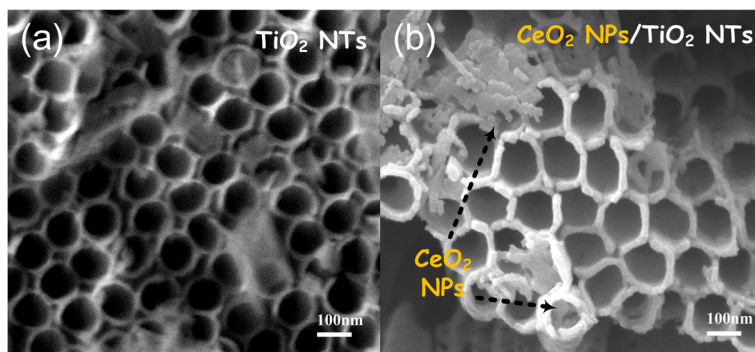


**Fig. 4** Typical SEM images of **a** pure TiO<sub>2</sub> nanotube arrays without modification and **b** the CeO<sub>2</sub>/TiO<sub>2</sub> heterojunction, indicating the highly ordered structure with open tube mouth morphology, and after modification, CeO<sub>2</sub> was successfully loaded into the TiO<sub>2</sub> nanotube arrays



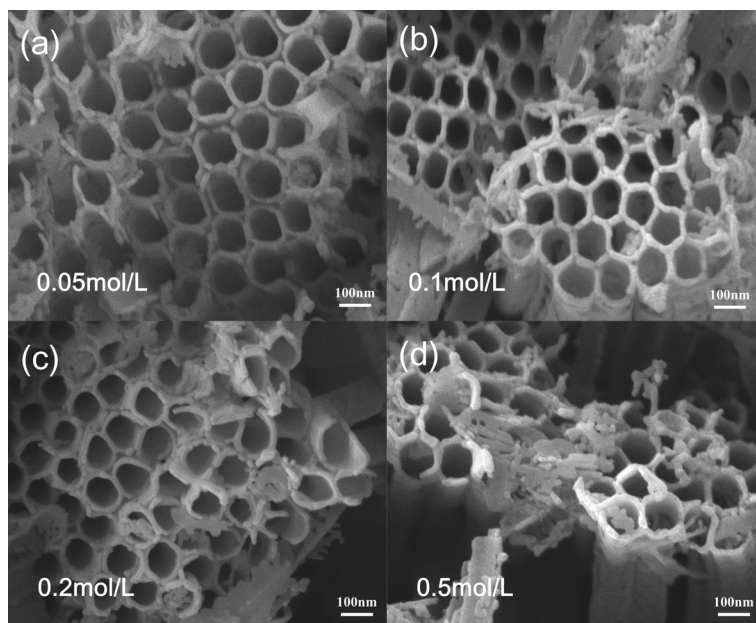


**Fig. 5** SEM images of the  $\text{CeO}_2/\text{TiO}_2$  heterojunctions with different  $\text{Ce}(\text{NO}_3)_3$  solution concentration: **a** sample immersed in 0.05 mol/L  $\text{Ce}(\text{NO}_3)_3$ ; **b** sample immersed in 0.1 mol/L  $\text{Ce}(\text{NO}_3)_3$ ; **c** sample immersed in 0.2 mol/L  $\text{Ce}(\text{NO}_3)_3$ ; and **d** sample immersed in 0.5 mol/L  $\text{Ce}(\text{NO}_3)_3$

#### Mechanism of the $\text{CeO}_2/\text{TiO}_2$ Heterojunction Formation

According to the reported studies, the most common used method for preparing  $\text{CeO}_2/\text{TiO}_2$  heterojunction is the sol-gel method or the secondary redox method [40]. In order to obtain the  $\text{CeO}_2/\text{TiO}_2$  heterojunction in a very simple procedure with low cost, in this paper, the preparation of  $\text{CeO}_2/\text{TiO}_2$  heterojunction is achieved by filling  $\text{TiO}_2$  NT nano-container with  $\text{Ce}(\text{NO}_3)_3$  solution and then thermal decomposition of  $\text{Ce}(\text{NO}_3)_3$ . The high temperature breaks the chemical bonds of  $\text{Ce}(\text{NO}_3)_3$

molecules, and the decomposed Ce, O, and N atoms then reform into  $\text{CeO}_2$  NPs and  $\text{NO}/\text{O}_2$ . This process is schematically shown as Fig. 8. Firstly, the  $\text{Ce}(\text{NO}_3)_3$  aqueous solution with different concentrations were filled into the  $\text{TiO}_2$  NT nano-container. Then, the film were baked at 70 °C for 1 h, during which  $\text{Ce}(\text{NO}_3)_3$  will be deposited from water in the form of  $\text{Ce}(\text{NO}_3)_3 \cdot 6\text{H}_2\text{O}$  and finally change into  $\text{Ce}(\text{NO}_3)_3$  loaded inside those  $\text{TiO}_2$  NT nano-container. Then, the  $\text{Ce}(\text{NO}_3)_3$ -loaded  $\text{TiO}_2$  NT films were annealed at a high temperature of

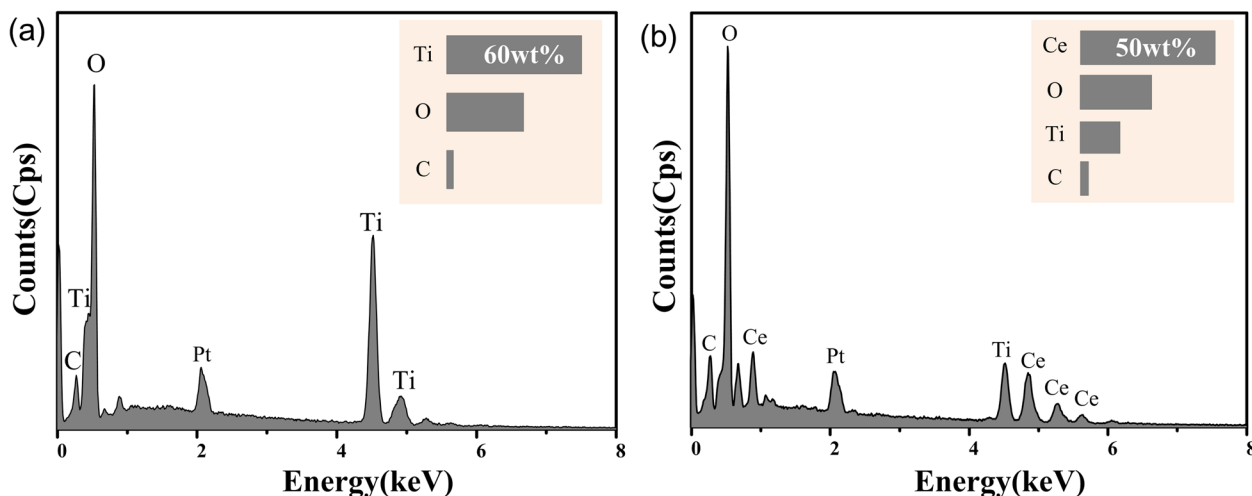


**Fig. 6** EDS results of **a** pure  $\text{TiO}_2$  NTs and **b**  $\text{CeO}_2/\text{TiO}_2$  heterojunction, showing the existence of element Ti, Ce, and O after loading  $\text{Ce}(\text{NO}_3)_3$ . The results confirm the successful loading of  $\text{CeO}_2$  on the  $\text{TiO}_2$  NTAs

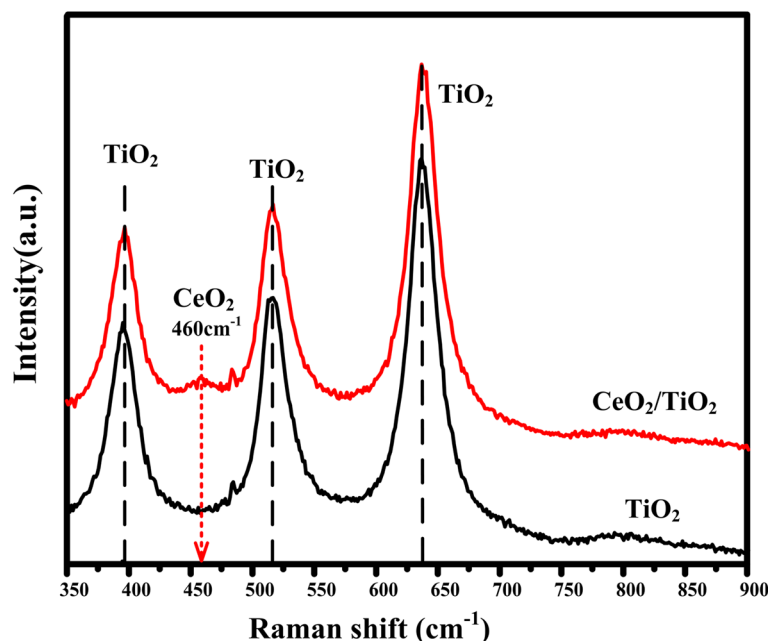
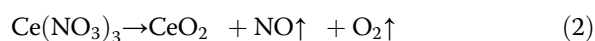
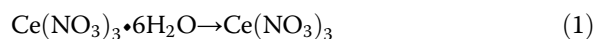


**Fig. 7** Raman spectra of pure TiO<sub>2</sub> NTs and CeO<sub>2</sub>/TiO<sub>2</sub> heterojunction, indicating CeO<sub>2</sub> NPs were successfully loaded into the TiO<sub>2</sub> NTAs

450 °C for 2 h. Under high temperature conditions, the chemical bonds in the Ce(NO<sub>3</sub>)<sub>3</sub> molecule will be broken and recombine, resulting in the generation of CeO<sub>2</sub> NPs inside the TiO<sub>2</sub> NTs. Two involved chemical reaction are expressed as following eq. (1) and (2):



In short, we have shown a facile method using TiO<sub>2</sub> NT nano-container to load Ce(NO<sub>3</sub>)<sub>3</sub> to prepare CeO<sub>2</sub>/TiO<sub>2</sub> heterojunction films. Ce(NO<sub>3</sub>)<sub>3</sub> thermal decomposition inside each individual anodic TiO<sub>2</sub> NTs allows for a

good formation and distribution of the CeO<sub>2</sub> NPs. CeO<sub>2</sub>/TiO<sub>2</sub> heterojunction films have lots of potential applications. In the field of photocatalysis, it can be used to degrade water pollution, because CeO<sub>2</sub> can inhibit the rapid electron-hole recombination of TiO<sub>2</sub> and the heterojunction films can adsorb organic pollutants efficiently. In the field of the photocatalytic hydrogen production and the improvement of TiO<sub>2</sub> oxygen sensor, CeO<sub>2</sub> NPs/TiO<sub>2</sub> NTA films can also be used well.

## Conclusions

Self-organized TiO<sub>2</sub> NT arrays were prepared through an electrochemistry process, and they were taken as nano-containers to load CeO<sub>2</sub> raw materials. After thermal

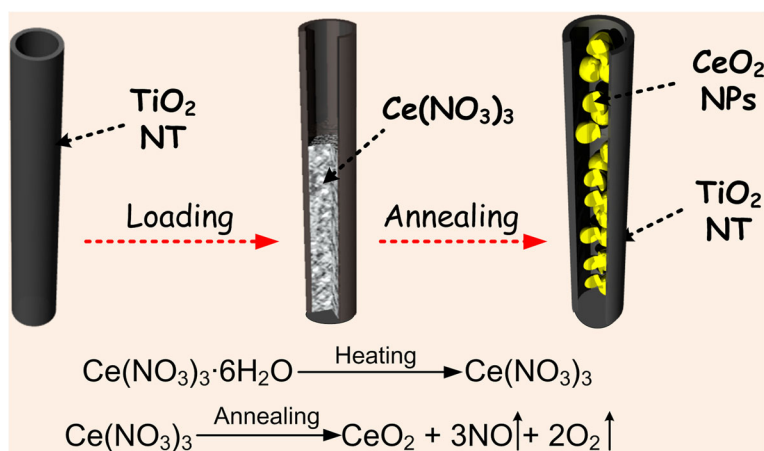


**Fig. 8** Schematic synthesis diagram of the CeO<sub>2</sub>/TiO<sub>2</sub> heterojunctions and involved chemical equations

treatment, well-distributed CeO<sub>2</sub> NPs were successfully obtained and loaded onto TiO<sub>2</sub> NT arrays, forming CeO<sub>2</sub>/TiO<sub>2</sub> heterojunction films. The formation of cubic CeO<sub>2</sub> and anatase TiO<sub>2</sub> were confirmed by XRD. Microscopic morphologies of different CeO<sub>2</sub>/TiO<sub>2</sub> heterojunction are characterized by SEM, which shows the CeO<sub>2</sub> NPs were tightly deposited both around the tube and inside the inner wall of the TiO<sub>2</sub> NT arrays. The successful preparation of CeO<sub>2</sub>/TiO<sub>2</sub> heterojunction films were also confirmed by EDS and Raman spectra. In summary, this study provides a simple method to prepare CeO<sub>2</sub>/TiO<sub>2</sub> heterojunction films with good morphology, heterogeneous stability, and low cost, which would be promising for environmental and energy-related applications.

#### Abbreviations

EDS: Energy-dispersive spectrometry; NT: Nanotube; SEM: Scanning electron microscopy; XRD: X-ray diffraction

#### Funding

This work was financially supported by the National R&D Program of China under No. 2017YFA0207400; National Key Research and Development Plan under No. 2016YFA0300801; National Natural Science Foundation of China under Nos. 51502033, 61571079, 61131005, and 51572042; National Basic Research Program of China under Grant No. 2012CB933104; 111 Project No. B13042; International Cooperation Projects under Grant No. 2015DFR50870; and the Science and Technology project of Sichuan Province No. 2017JY0002.

#### Availability of Data and Materials

They are all in the main text and figures.

#### Authors' Contributions

YL conceived and supervised the research. BY conducted the experiments and wrote the manuscript. DZ, XW, YL, QW, HZ, and ZZ made the theoretical analysis. All the authors discussed the results. All authors read and approved the final manuscript.

#### Competing Interests

The authors declare that they have no competing interests.

#### Publisher's Note

Springer Nature remains neutral with regard to jurisdictional claims in published maps and institutional affiliations.

Received: 26 January 2018 Accepted: 27 March 2018

Published online: 03 April 2018

#### References

- Gratzel M (2001) Photoelectrochemical cells. *Nature* 414:338–344
- Linsebigler AL, Lu GQ, Yates JT (1995) Photocatalysis on TiO<sub>2</sub> surfaces—principles, mechanisms, and selected results. *Chem Rev* 95:735–758
- Nakajima A, Fujishima A, Hashimoto K, Watanabe T (1999) Preparation of transparent superhydrophobic boehmite and silica films by sublimation of aluminum acetylacetonate. *Adv Mater* 11:1365–1368
- Fujishima A, Rao TN, Tryk DA (2000) TiO<sub>2</sub> photocatalysts and diamond electrodes. *Electrochim Acta* 45:4683–4690
- Oregan B, Gratzel M (1991) A low-cost, high-efficiency solar-cell based on dye-sensitized colloidal TiO<sub>2</sub> films. *Nature* 353:737–740
- Khan MM, Ansari SA, Pradhan D, Ansari MQ, Han DH, Lee J, Cho MH (2014) Band gap engineered TiO<sub>2</sub> nanoparticles for visible light induced photoelectrochemical and photocatalytic studies. *J Mater Chem A* 2:637–644
- Kholmanov IN, Barborini E, Vinati S, Piseri P, Podesta A, Ducati C, Lenardi C, Milani P (2003) The influence of the precursor clusters on the structural and morphological evolution of nanostructured TiO<sub>2</sub> under thermal annealing. *Nanotechnology* 14:1168–1173
- Ong WJ, Tan LL, Chai SP, Yong ST, Mohamed AR (2014) Highly reactive {001} facets of TiO<sub>2</sub>-based composites: synthesis, formation mechanism and characterization. *Nano* 6:1946–2008
- Wang MY, Iocozia J, Sun L, Lin CJ, Lin ZQ (2014) Inorganic-modified semiconductor TiO<sub>2</sub> nanotube arrays for photocatalysis. *Energy Environ Sci* 7:2182–2202
- Nolan NT, Seery MK, Pillai SC (2009) Spectroscopic investigation of the anatase-to-rutile transformation of sol-gel-synthesized TiO<sub>2</sub> photocatalysts. *J Phys Chem C* 113:16151–16157
- Reddy KR, Hassan M, Gomes VG (2015) Hybrid nanostructures based on titanium dioxide for enhanced photocatalysis. *Applied Catalysis a-General* 489:1–16
- Gong D, Grimes CA, Varghese OK, Hu WC, Singh RS, Chen Z, Dickey EC (2001) Titanium oxide nanotube arrays prepared by anodic oxidation. *J Mater Res* 16:3331–3334
- Grimes CA (2007) Synthesis and application of highly ordered arrays of TiO<sub>2</sub> nanotubes. *J Mater Chem* 17:1451–1457
- Lai Y, Gao X, Zhuang H, Huang J, Lin C, Jiang L (2009) Designing superhydrophobic porous nanostructures with tunable water adhesion. *Adv Mater* 21:3799–3803
- Macak JM, Schmuki P (2006) Anodic growth of self-organized anodic TiO<sub>2</sub> nanotubes in viscous electrolytes. *Electrochim Acta* 52:1258–1264
- Roy P, Berger S, Schmuki P (2011) TiO<sub>2</sub> nanotubes: synthesis and applications. *Angewandte Chemie-International Edition* 50:2904–2939
- He ZL, Que WX, He YC, Hu JX, Chen J, Javed HMA, Ji YN, Li XN, Fei D (2013) Electrochemical behavior and photocatalytic performance of nitrogen-doped TiO<sub>2</sub> nanotubes arrays powders prepared by combining anodization with solvothermal process. *Ceram Int* 39:5545–5552
- He Z, Kim C, Lin LH, Jeon TH, Lin S, Wang XC, Choi W (2017) Formation of heterostructures via direct growth CN on h-BN porous nanosheets for metal-free photocatalysis. *Nano Energy* 42:58–68
- Park JH, Kim S, Bard AJ (2006) Novel carbon-doped TiO<sub>2</sub> nanotube arrays with high aspect ratios for efficient solar water splitting. *Nano Lett* 6:24–28
- Woan K, Pyrgiotakis G, Sigmund W (2009) Photocatalytic carbon-nanotube-TiO<sub>2</sub> composites. *Adv Mater* 21:2233–2239
- Zheng Q, Zhou B, Bai J, Li L, Jin Z, Zhang J, Li J, Liu Y, Cai W, Zhu X (2008) Self-organized TiO<sub>2</sub> nanotube array sensor for the determination of chemical oxygen demand. *Adv Mater* 20:1044–1049
- Liao Y, Brame J, Que W, Xiu Z, Xie H, Li Q, Fabian M, Alvarez PJ (2013) Photocatalytic generation of multiple ROS types using low-temperature crystallized anodic TiO<sub>2</sub> nanotube arrays. *J Hazard Mater* 260:434–441
- Rajeshwar K, Osugi ME, Chanmanee W, Chenthamarakshan CR, Zaroni MVB, Kajitvichyanukul P, Krishnan-Ayer R (2008) Heterogeneous photocatalytic treatment of organic dyes in air and aqueous media. *Journal Of Photochemistry And Photobiology C-Photochemistry Reviews* 9:171–192
- Masmoudi O, Boureau G, Nacer B, Benzakour M, Millot F, Tetot R (1991) Influence of the coulomb forces on the thermodynamic and transport-properties of nonstoichiometric cerium dioxide. *Radiation Effects And Defects In Solids* 119:803–808
- Trinchi A, Li YX, Wlodarski W, Kaciulis S, Pandolfi L, Viticoli S, Comini E, Sberveglieri G (2003) Investigation of sol-gel prepared CeO<sub>2</sub>-TiO<sub>2</sub> thin films for oxygen gas sensing. *Sensors And Actuators B-Chemical* 95:145–150
- Ameen S, Akhtar MS, Seo HK, Shin HS (2014) Solution-processed CeO<sub>2</sub>/TiO<sub>2</sub> nanocomposite as potent visible light photocatalyst for the degradation of bromophenol dye. *Chem Eng J* 247:193–198
- Contreras-Garcia ME, Garcia-Benjume ML, Macias-Andres VI, Barajas-Ledesma E, Medina-Flores A, Espitia-Cabrera MI (2014) Synergic effect of the TiO<sub>2</sub>-CeO<sub>2</sub> nanoconjugate system on the band-gap for visible light photocatalysis. *Mater Sci Eng B* 183:78–85
- Avellaneda CO, Pawlicka A (1998) Preparation of transparent CeO<sub>2</sub>-TiO<sub>2</sub> coatings for electrochromic devices. *Thin Solid Films* 335:245–248
- Karunakaran C, Navamani P, Gomathisankar P (2015) Particulate sol-gel synthesis and optical and electrical properties of CeO<sub>2</sub>/TiO<sub>2</sub> nanocomposite. *J Iran Chem Soc* 12:75–80
- Macak JM, Zlamal M, Krysa J, Schmuki P (2007) Self-organized TiO<sub>2</sub> nanotube layers as highly efficient photocatalysts. *Small* 3:300–304
- Pavasupree S, Suzuki Y, Yoshikawa S, Kawahata R (2005) Synthesis of titanate, TiO<sub>2</sub>, and anatase TiO<sub>2</sub> nanofibers from natural rutile sand. *J Solid State Chem* 178:3110–3116
- Wang PH, Tang YX, Dong ZL, Chen Z, Lim TT (2013) Ag-AgBr/TiO<sub>2</sub>/RGO nanocomposite for visible-light photocatalytic degradation of penicillin G. *J Mater Chem A* 1:4718–4727

33. Wang SL, Qian HH, Hu Y, Dai W, Zhong YJ, Chen JF, Hu X (2013) Facile one-pot synthesis of uniform  $\text{TiO}_2$ -Ag hybrid hollow spheres with enhanced photocatalytic activity. *Dalton Trans* 42:1122–1128
34. He ZL, Que WX, Sun P, Ren JB (2013) Double-layer electrode based on  $\text{TiO}_2$  nanotubes arrays for enhancing photovoltaic properties in dye-sensitized solar cells. *ACS Appl Mater Interfaces* 5:12779–12783
35. Li L, Liu X, Zhang YL, Nuhfer NT, Barmak K, Salvador PA, Rohrer GS (2013) Visible-light photochemical activity of heterostructured core-shell materials composed of selected ternary titanates and ferrites coated by  $\text{TiO}_2$ . *ACS Appl Mater Interfaces* 5:5064–5071
36. Verma A, Joshi AG, Bakhshi AK, Shivaprasad SM, Agnihotry SA (2006) Variations in the structural, optical and electrochemical properties of  $\text{CeO}_2$ - $\text{TiO}_2$  films as a function of  $\text{TiO}_2$  content. *Appl Surf Sci* 252:5131–5142
37. Yue L, Zhang XM (2008) Preparation of highly dispersed  $\text{CeO}_2/\text{TiO}_2$  core-shell nanoparticles. *Mater Lett* 62:3764–3766
38. Jiang BT, Zhang SY, Guo XZ, Jin BK, Tian YP (2009) Preparation and photocatalytic activity of  $\text{CeO}_2/\text{TiO}_2$  interface composite film. *Appl Surf Sci* 255:5975–5978
39. Lu XW, Li XZ, Qian JC, Miao NM, Yao C, Chen ZG (2016) Synthesis and characterization of  $\text{CeO}_2/\text{TiO}_2$  nanotube arrays and enhanced photocatalytic oxidative desulfurization performance. *J Alloys Compd* 661:363–371
40. Koo B, Patel RN, Korgel BA (2009) Synthesis of  $\text{CuInSe}_2$  nanocrystals with trigonal pyramidal shape. *J Am Chem Soc* 131:3134–3135

**Submit your manuscript to a SpringerOpen<sup>®</sup> journal and benefit from:**

- Convenient online submission
- Rigorous peer review
- Open access: articles freely available online
- High visibility within the field
- Retaining the copyright to your article

---

Submit your next manuscript at ► [springeropen.com](https://www.springeropen.com)